The Effect of a Hydroxyapatite-Reinforced Polyethylene Stress Distributor in a Dental Implant on Compressive Stress Levels in Surrounding Bone

Osama A. Abu-Hammad, BDS, MSc, PhD[1]/Alan Harrison, TD, BDS, PhD, FDS, RCS[2]/
David Williams, BDS, BSc, PhD[3]

This study investigated various designs of stress breakers incorporated into the dental implant using 3-D finite element analysis. These designs employed hydroxyapatite-reinforced polyethylene (HRP), a material capable of inducing osseointegration. The most successful design was that of a dental implant with a peripheral HRP component that was in direct contact with the bone surrounding the neck of the implant. This design lowered the compressive stress values in bone around the neck of the implant. Attempts were also made to optimize this design. (INT J ORAL MAXILLOFAC IMPLANTS 2000;15:559–564)

Key words: *dental implants, dental models, dental stress analysis, finite element analysis, polyethylenes*

The term "stress breakers" with respect to dental implants denotes the components used to reduce stresses in the surrounding bone. Originally, this term was used in conjunction with removable partial dentures. A number of studies, eg, Chapman and Kirsch,[1] have recommended the incorporation of internal stress-breaking elements into dental implants and reported lower stress levels around those implants incorporating stress breakers. However, this phenomenon has been attributed to lower occlusal force levels associated with this type of implant design.

In almost all the dental implant systems that utilize stress breakers, the designs have included a component that allows differential movement between the abutment and the implant.[2–6] This movement is claimed to decrease the stresses in bone around the implant.[7,8] However, there is an increasing weight of evidence from recent studies that this arrangement is not effective in reducing bone stresses and may result in higher stresses than with all-titanium implants.[9–12]

This study, using 3-D finite element stress analysis, aims to investigate the effect of different stress breaker designs on the values of compressive stresses at the crestal bone around the neck of the implant.

MATERIALS AND METHODS

Five finite element models were generated, each describing a hollow cylindric dental implant 3.45 mm in diameter with a 10-mm-long osseointegrated portion placed in a cylindric block of bone 20 mm in diameter and 12 mm in height. In model 1 (Fig 1), the implant was constructed entirely from titanium. In models 2 to 5, the implants were modified to include hydroxyapatite-reinforced polyethylene (HRP), an elastic composite material that has the ability to osseointegrate.[13,14] This material was included at the neck region of the implants (Figs 2 to 4). The complete interface between the implant, including the elastic portion, was modeled as being osseointegrated. This was achieved by merging together the common nodes between the implant and the surrounding bone. The Young's modulus of elasticity (ε) and Poisson's ratio (ν) of the materials used in this study are presented in Table 1.

[1]Postgraduate Student, Department of Oral and Dental Science, Dental School, University of Bristol, Bristol, United Kingdom.
[2]Professor and Head, Department of Oral and Dental Science, Dental School, University of Bristol, Bristol, United Kingdom.
[3]Lecturer, Department of Oral and Dental Science, Dental School, University of Bristol, Bristol, United Kingdom.

Reprint requests: Professor Alan Harrison, Department of Oral and Dental Science, Dental School and Hospital, Lower Maudlin Street, Bristol BS1 2LY, United Kingdom. Fax: +44-117-9284780.

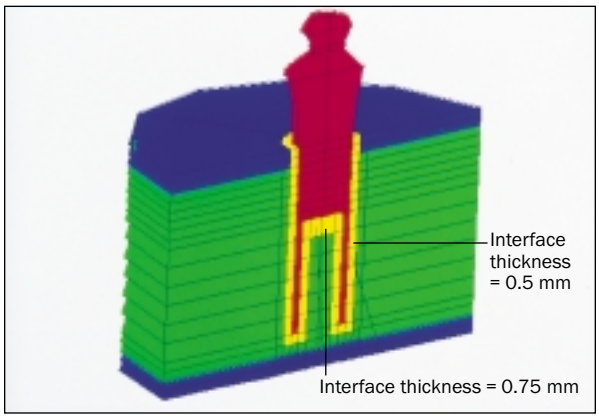

Fig 1 Model 1 (control implant): vertical section showing the relationship of the implant to the cylindric bony block. Note the restrained nodes at the sides of the model and the direction of the applied loads at the top of the implant. Blue = cortical bone; green = trabecular bone.

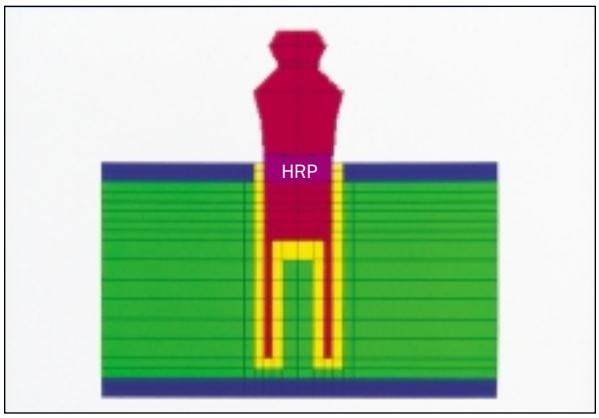

Fig 2 Model 2: vertical section showing the relationship of the implant to the cylindric bony block. Note the elastic material (HRP) incorporated into the design of the implant at the neck region.

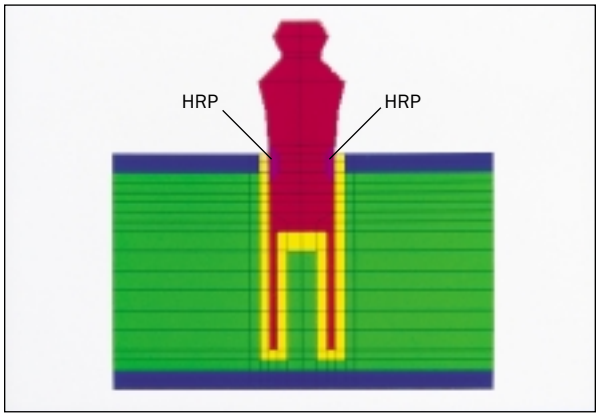

Fig 3 Model 3: vertical section showing the relation of the implant to the cylindric bony block. Note the elastic material (HRP) incorporated peripherally into the design of the implant at the neck region.

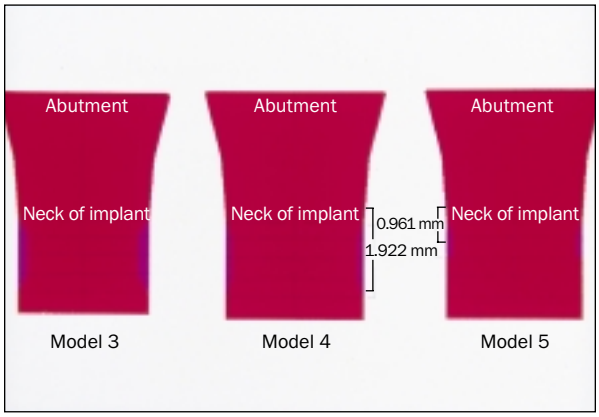

Fig 4 Vertical sections showing the neck region of implant models 3, 4, and 5. The thickness of the HRP in implant model 3 is 0.25 mm, whereas in models 4 and 5 the thickness is 0.125 mm. Purple = HRP; red = titanium.

Table 1 Material Properties of the Various Parts of the Finite Element Models

Material	Young's modulus (ε) (MPa)	Poisson's ratio (ν)
Titanium	103,400	0.35
Cortical bone	13,700	0.3
Trabecular bone	1370	0.3
Interface bone	13,700	0.3
HRP	8000	0.3

In the second model (Fig 2), the properties of the section of the implant and abutment passing through the upper cortical plate were changed from those of titanium to those of the HRP material (ε= 8,000 MPa).

In the third model (Figs 3 and 4), the neck of the implant was modeled as a central titanium core with a peripheral (HRP) component 0.25 mm thick. The length of the component in model 4 was 1.922 mm, and in model 5 the length was 0.961 mm (Fig 4).

A layer of interface bone 0.5 mm thick covered the surface of the hollow cylindric implants, both externally and internally. The interface bone at the base of the inside of the cylinder was modeled to be 0.75 mm thick (Figs 1 to 3). Each implant, with its surrounding interface, was modeled as though placed in a cylindric block of bone 20 mm in diameter and 12 mm in height. Each block of bone was modeled with upper and lower cortical plates 1 mm thick, with the remainder as cancellous bone (Figs 1 to 3). As illustrated in Fig 1, all the nodes at the sides of the models were restrained, and 2 loading cases were modeled, applied at the top middle node of the implants. The first was a 100 N vertical load downward along the long axis of the implant, and the second was a horizontal load of 100 N perpendicular to

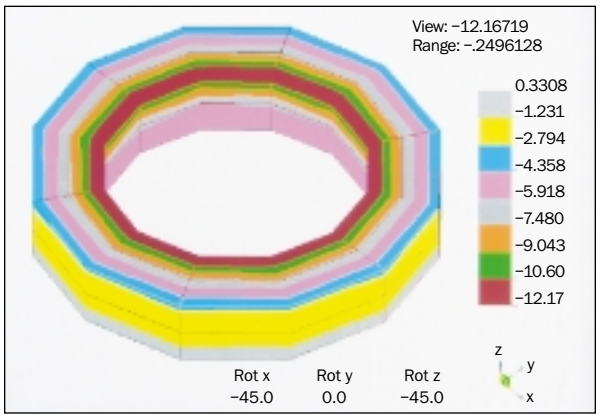

Fig 5 Model 1 (control implant) under vertical loading. Compressive (third principal) stress distribution at the top 1 mm of the interface zone around the neck of the implant (without stress breaker).

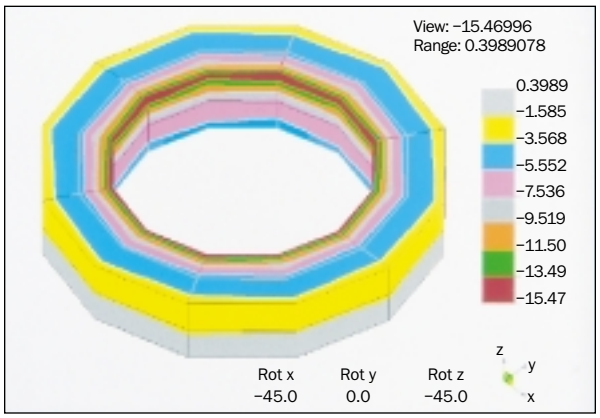

Fig 6 Model 2 under vertical loading. Compressive (third principal) stress distribution at the top 1 mm of the interface zone around the neck of the implant (with stress breaker).

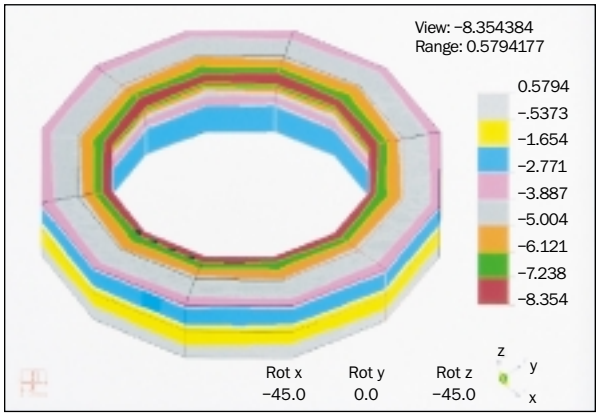

Fig 7 Model 3 under vertical loading. Compressive (third principal) stress distribution at the top 1 mm of the interface zone around the neck of the implant (with stress breaker).

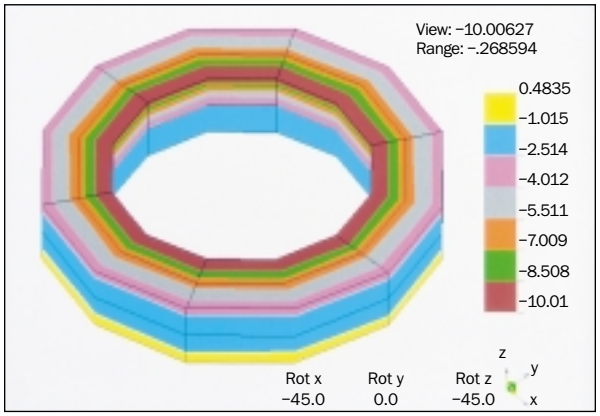

Fig 8 Model 4 under vertical loading. Compressive (third principal) stress distribution at the top 1 mm of the interface zone around the neck of the implant (with stress breaker).

the long axis of the implant (the direction was irrelevant, as the structure was axisymmetric).

Linear finite element modeling was used for the investigation since bone-implant integration was assumed, ie, a perfect bond between bone and implant. If a less-than-perfect bond was assumed, then contact analysis (non-linear) might be considered more appropriate. There is, however, considerable evidence to support the supposition that there is true bone-implant integration and not simply bone apposition against the surface of the implant.

RESULTS

A pictorial representation was obtained of the third principal stress in the bone around the necks of the implants in all models, under vertical and horizontal loading (Figs 5 to 14). To reveal the stress patterns

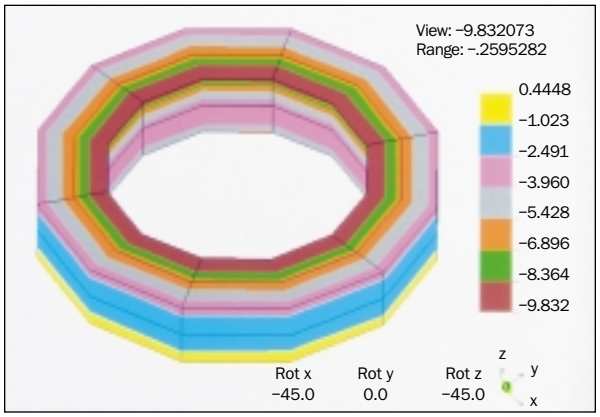

Fig 9 Model 5 under vertical loading. Compressive (third principal) stress distribution at the top 1 mm of the interface zone around the neck of the implant (with stress breaker).

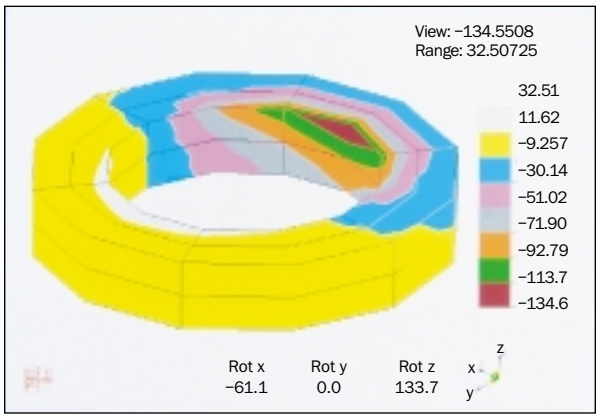

Fig 10 Model 1 (control implant) under horizontal loading. Compressive (third principal) stress distribution at the top 1 mm of the interface zone around the neck of the implant (without stress breaker).

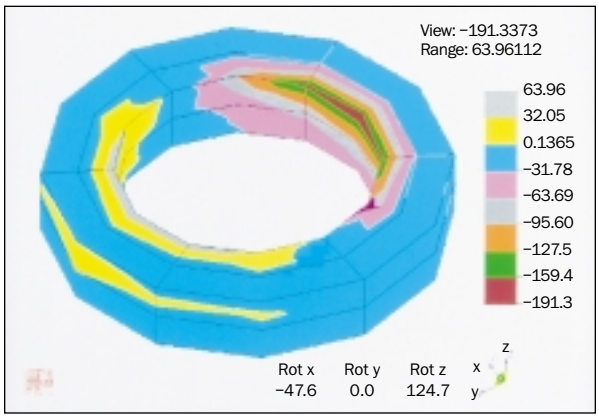

Fig 11 Model 2 under horizontal loading. Compressive (third principal) stress distribution at the top 1 mm of the interface zone around the neck of the implant (with stress breaker).

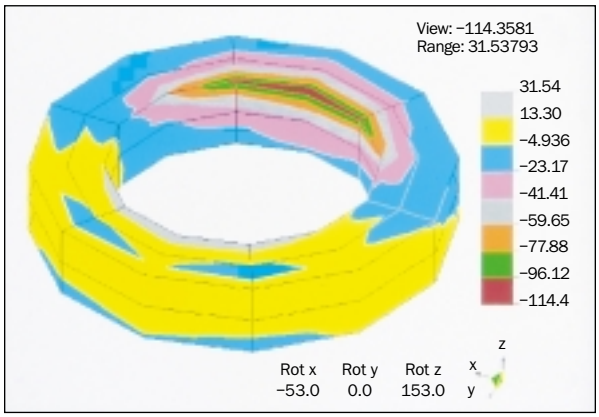

Fig 12 Model 3 under horizontal loading. Compressive (third principal) stress distribution at the top 1 mm of the interface zone around the neck of the implant (with stress breaker).

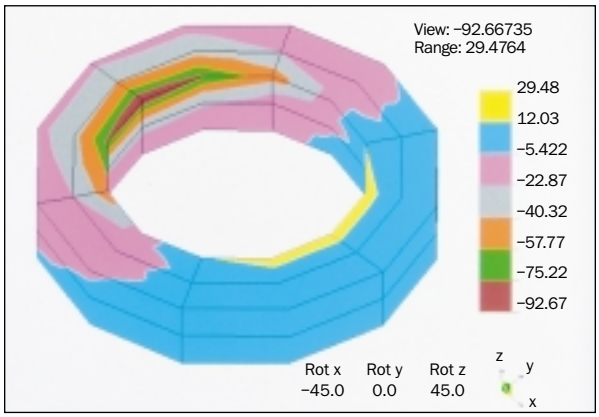

Fig 13 Model 4 under horizontal loading. Compressive (third principal) stress distribution at the top 1 mm of the interface zone around the neck of the implant (with stress breaker).

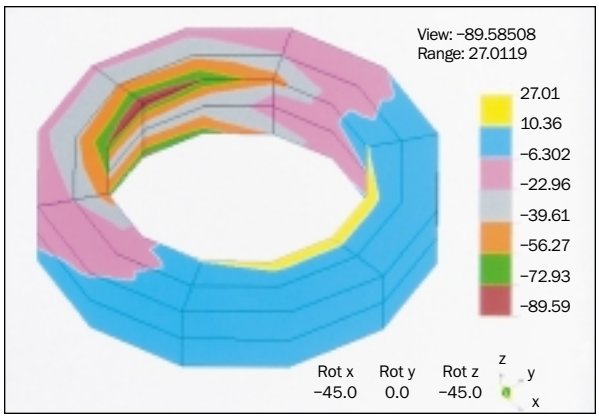

Fig 14 Model 5 under horizontal loading. Compressive (third principal) stress distribution at the top 1 mm of the interface zone around the neck of the implant (with stress breaker).

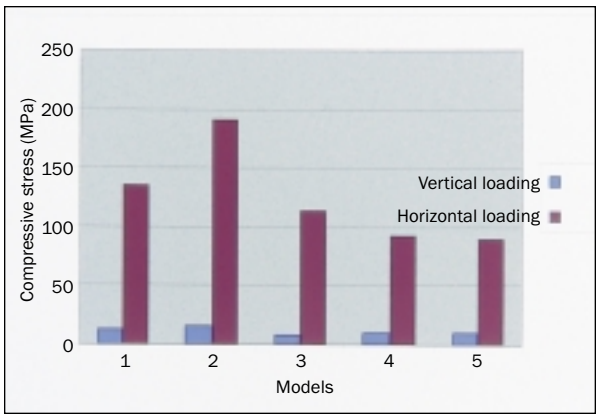

Fig 15 Maximal compressive (third principal) stresses at the interface bone for the 5 implant models under vertical and horizontal loading.

without obstruction, the implant has been omitted. The maximum stress levels in all models are recorded in Table 2. Maximum stress values in bone appear to be concentrated superiorly in the cortical bone closest to the implants.

In the first 3 models, the stress values under vertical loading were 12.17 MPa, 15.47 MPa, and 8.354 MPa, respectively. The highest value was found in implant model 2 (15.47 MPa), whereas the lowest value was found in implant model 3 (8.354 MPa). In models 4 and 5, the corresponding values were 10.01 MPa and 9.832 MPa, which are lower than the values for the all-titanium implant but higher than those for model 3.

In models 1 to 3, the highest stress values under horizontal loading were observed in implant model 2 (191.3 MPa) and the lowest were seen in implant model 3 (114.4 MPa). Corresponding stress values in models 4 and 5 show even lower stress values than those in model 3.

The stress-breaker design used in implant model 2 resulted in higher stress values at the neck of the implant on vertical and horizontal loading of the implant than in implant model 1, with stress values that were 29.4% and 42.1% higher than those for vertical and horizontal loading, respectively. However, the stress-breaker design in implant model 3 resulted in lower stresses under both vertical and horizontal loading compared to implant model 1, with stresses 31.4% and 15% lower under vertical and horizontal loading, respectively. This is illustrated in Fig 15.

Table 2 Maximal Stress Recordings at Coronal 2 mm of Interface Bone Under Vertical and Horizontal Loading in All Models

	Third principal stress (MPa)	
Model	Vertical loading	Horizontal loading
1	12.17	134.6
2	15.47	191.3
3	8.354	114.4
4	10.01	92.67
5	9.832	89.59

DISCUSSION

The results of this study suggest that it is possible for a stress-breaker that is built into the geometry of the implant to lower the compressive stress levels in the bone around the collar of the implant. It is argued that it is the high stress levels in that region that are responsible for bone resorption around the neck of an implant.

Incorporation of the HRP material into the geometry of the implant such that it contacts the bone can be acceptable, since the material is capable of inducing osseointegration.[13] In this study, 2 experimental stress-breaker designs were modeled and compared to a control implant without a stress breaker. It can be seen that where the entire section of the implant was modeled with HRP material, the compressive (third principal) stresses generated on vertical and horizontal loading exceeded the corresponding stresses for the control.

These results may be explained as follows. With vertical loading of the implant, the elastic material at the neck region bulges sideways against the bone around the neck of the implant because of the pressure on the abutment above and the resistance from the implant below. This bulging will result in more and higher stresses. On horizontal loading, as a result of its elasticity, the material will bend against the marginal bone, and loads will be largely distributed to this section of bone. It appears that the HRP material with this arrangement fails to transmit loads from the abutment downward to the implant.

In the third design, the central elements of the neck of the implant were modeled as titanium and only the peripheral elements were modeled as HRP. This design resulted in lower compressive stress values for vertical and horizontal loading versus the control. These results indicate that the central titanium core of the implant transmitted part of the load downward to the implant, while the peripheral material in contact with the surrounding bone exerted small forces and produced a cushioning effect, especially during horizontal loading.

Rieger et al[15] tested the effect of implant geometry on stress distribution in bone around it and suggested that for all geometries tested, increasing the stiffness of the material transmitted more of the occlusal load to the apical bone. This seems to be an appropriate explanation for the reduction of stresses that occurred in relation to the implant with the second stress-breaker design in the present study.

Models 4 and 5 represent attempts to further modify the design in model 3 by maintaining the contact with bone and reducing the thickness and length of the material. However, this resulted in higher stresses under vertical loading but lower stresses under horizontal loading of these implants when compared to implant model 3. The reduction in model 4 was some 19% of the stress value for model 3 under horizontal loading.

Since the material used (hydroxyapatite-reinforced polyethylene) was biocompatible,[13] its surfaces in contact with bone will osseointegrate. This was represented in the model in the present study by merging the nodes common between this material and surrounding bone.

Changing the pattern of restraints in the model will affect the stress values but generally not the pattern of distribution. The block of bone modeled does not represent the mandible or maxilla. However, it is the same throughout all the models, and comparisons can therefore be made. The aim of the study was not to explore the exact distribution of stresses in the arches or to register the values of stresses in humans, but to compare the different implant/stress-breaker designs. Off-axis loading was not attempted, as this type of loading can always be analyzed via the 2 components—vertical and horizontal. Analysis of each in turn simplifies the issue, and a combination of these 2 types of loads only serves to complicate analysis and mask important phenomena, such as the higher stresses produced in the system under horizontal loading when compared to vertical forces.

If vertical bone loss was assumed to occur around the neck of the implant so that the bone does not come into contact with the stress-breaking mechanism, then that mechanism will not function and stress levels will again be similar to those of a standard implant. This study did not investigate the effect of less than 100% coverage of bone over the full length of the implant, as this can be considered another of many possible variables. However, it did attempt to establish that it is possible to reduce the stresses around an implant by varying its geometry and components.

CONCLUSIONS

- Bone stresses under horizontal loading are more severe than under vertical loading and are generally about 10 times their value.
- Hydroxyapatite-reinforced polyethylene can reduce stresses around the neck of the implant if embedded in the implant design as an O-ring of various cross sections.
- Stresses tend to be lower if the O-ring is thin and extended to no more than the top part of the crestal bone around the neck of the implant.

REFERENCES

1. Chapman RJ, Kirsch A. Variations in occlusal forces with a resilient internal implant shock absorber. Int J Oral Maxillofac Implants 1990;5:369–374.
2. Siegele D, Soltész U. Dental implants with flexible inserts—A possibility to improve stress distribution in the jaw. In: Perren SM, Schneider E (eds). Biomechanics: Current Interdisciplinary Research. Dordrecht: M. Nihoff, 1985:271–276.
3. Mentag PJ, Kosinski T. Hydroxyapatite-augmented sites as receptors for replacement implants. J Oral Implantol 1980; 15:114–123.
4. Uysal H, Iplikcioglu H, Avci M, Bilir OG, Kural O. Efficacy of the intramobile connector in implant tooth-supported fixed prostheses: An experimental stress analysis. Int J Prosthodont 1996;9:355–361.
5. Uysal H, Iplikcioglu H, Avci M, Bilir OG, Kural O. An experimental analysis of the stresses on the implant in an implant-tooth-supported prosthesis: A technical note. Int J Oral Maxillofac Implants 1997;12:118–124.
6. Haganman CR, Holmes DC, Aquilino SA, Diaz-Arnold AM, Stanford CM. Defection and stress distribution in three different IMZ abutment designs. J Prosthodont 1997;6: 110–121.
7. Kraut RA, Kirsch A. Practical stress absorption by means of modified abutments. Case presentations. Pract Periodontics Aesthet Dent 1993;5:67–74.
8. Clift SE, Fisher J, Edwards BN. Comparative analysis of bone stresses and strains in the Intoss dental implant with and without a flexible internal post. Proc Inst Mech Eng 1995;209:139–147.
9. McGlumphy EA, Campagni WV, Peterson LJ. A comparison of the stress transfer characteristics of a dental implant with a rigid or a resilient internal element. J Prosthet Dent 1989;62:586–593.
10. Van Rossen IP, Braak LH, de Putter C, de Groot K. Stress-absorbing elements in dental implants. J Prosthet Dent 1990;64:198–205.
11. Holmes DC, Grigsby WR, Goel VK, Keller JC. Comparison of stress transmission in the IMZ implant system with polyoxymethylene or titanium intramobile element: A finite element stress analysis. Int J Oral Maxillofac Implants 1992; 7:450–458.
12. Holmes DC, Haganman CR, Aquilino SA. Deflection of superstructure and stress concentrations in the IMZ implant system. Int J Prosthodont 1994;7:239–246.
13. Hobkirk JA. Endosseous implants: The host-implant surface [review]. Ann Acad Med Singapore 1986;15:403–408.
14. Wolfe LA, Hobkirk JA. Bone response to a matched modulus endosseous implant material. Int J Oral Maxillofac Implants 1989;4:311–320.
15. Rieger MR, Fareed K, Adams WK, Tanquist RA. Bone stress distribution for three endosseous implants. J Prosthet Dent 1989;61:223–228.